Acute Lipopolysaccharide-Mediated Injury in Neonatal White Matter Glia: Role of TNF- α, IL-1 β, and Calcium

Catherine Sherwin and Robert Fern

J Immunol 2005; 175:155-161; ;
http://www.jimmunol.org/content/175/1/155

The Journal of Immunology is published twice each month by
The American Association of Immunologists, Inc.,
9650 Rockville Pike, Bethesda, MD 20814-3994.

Print ISSN: 0022-1767 Online ISSN: 1550-6606.

Acute Lipopolysaccharide-Mediated Injury in Neonatal White Matter Glia: Role of TNF-α, IL-1β, and Calcium[1]

Catherine Sherwin and Robert Fern[2]

Bacterial infection is implicated in the selective CNS white matter injury associated with cerebral palsy, a common birth disorder. Exposure to the bacterial endotoxin LPS produced death of white matter glial cells in isolated neonatal rat optic nerve (RON) (a model white matter tract), over a 180-min time course. A delayed intracellular Ca^{2+} concentration ($[Ca^{2+}]_i$) rise preceded cell death and both events were prevented by removing extracellular Ca^{2+}. The cytokines TNF-α or IL-1β, but not IL-6, mimicked the cytotoxic effect of LPS, whereas blocking either TNF-α with a neutralizing Ab or IL-1 with recombinant antagonist prevented LPS cytotoxicity. Ultrastructural examination showed wide-scale oligodendroglial cell death in LPS-treated rat optic nerves, with preservation of astrocytes and axons. Fluorescently conjugated LPS revealed LPS binding on microglia and astrocytes in neonatal white and gray matter. Astrocyte binding predominated, and was particularly intense around blood vessels. LPS can therefore bind directly to developing white matter astrocytes and microglia to evoke rapid cell death in neighboring oligodendroglia via a calcium- and cytokine-mediated pathway. In addition to direct toxicity, LPS increased the degree of acute cell death evoked by ischemia in a calcium-dependent manner. *The Journal of Immunology,* **2005, 175: 155–161.**

Cerebral palsy is a common human birth disorder manifest in the first years of life, which continues unabated throughout the lifetime of the patient. There is currently no effective remedy or prophylactic strategy (1–3). In the majority of cases, cerebral palsy involves a lesion centered upon the developing white matter adjacent to the ventricles (periventricular leukomalacia (PVL)[3]). PVL arises in mid-gestation at a point when myelination is initiating (4). Injury of white matter glial cells is prevalent and may involve selective loss of oligodendroglia with subsequent hypomyelination (5–7).

An increasing number of studies have implicated intrauterine infection and chorioamnionitis in the genesis of PVL. Early reports demonstrated that i.v. injection of the bacterial endotoxin LPS can produce selective white matter injury in neonatal CNS (8, 9). Recent studies have shown that direct LPS injection into the developing brain can evoke white matter damage (10, 11), whereas induction of intrauterine infection can produce diffuse glial cell death and cavitation in fetal white matter (12, 13). The mechanism of LPS cytotoxicity in developing white matter appears to involve cell-cell interactions. For example, cultured oligodendroglia die when exposed to LPS provided that other glial types are present (14–17), whereas media collected from LPS-treated microglia or astrocytes is toxic to oligodendroglia in culture (15, 18). A recent report suggests that microglia are the only neural cell type to express the LPS receptor TLR-4, although this has not been examined in vivo (17).

LPS can promote the release of cytokines from glia, whereas cytokine production is implicated in the association between intrauterine infection, preterm birth and neonatal brain damage (see *Discussion*). However, because i.v. injection of LPS produces systemic hypotension (19), whereas chorioamnionitis is associated with hypotension in the fetus (20), it is uncertain whether bacterial infection produces white matter injury as a direct effect, or subsequent to ischemia associated with hypotension. Experimental studies have repeatedly demonstrated that immature white matter is predisposed to ischemia during hypotension, and is highly sensitive to ischemic injury (1). The immature oligodendroglia that populate white matter at this age are exquisitely sensitive to ischemic injury (21, 22). The current study examines LPS-mediated cytotoxicity in glial cells in isolated white matter, to establish the potential for direct LPS-mediated white matter injury independent of hemodynamic factors. The mechanism and characteristics of direct LPS cytotoxicity are investigated and the pattern of glial cell binding of LPS examined in situ.

Materials and Methods

Optic nerves were dissected from P8-P12 (called "P10" throughout) Lister hooded rats and placed in artificial cerebrospinal fluid (aCSF) composed (in mM) 153 Na^+, 3 K^+, 2 Mg^{2+}, 2 Ca^{2+}, 131 Cl^-, 26 HCO_3^-, 2 $H_2PO_4^-$, 10 dextrose, bubbled with 95% O_2/5% CO_2. All procedures involving the use of animals were approved by local ethical review. At this age, the rat optic nerve (RON) is initiating the process of myelination, with the first wraps of myelin appearing (23, 24). This is the same developmental point at which periventricular white matter is subject to PVL in the fetus (4, 25).

Bacterial LPS (from *Escherichia coli*; Sigma-Aldrich) was dissolved in aCSF immediately before the experiment to give a final concentration of 1 μg/ml. Ischemia was induced by changing from aCSF to perfusion with zero-glucose aCSF that had been bubbled with 95% N_2/5% CO_2 for at least 60 min. The atmosphere in the recording chamber was switched simultaneously to 95% N_2/5% CO_2 (see Ref. 26 for further details). Ischemia was maintained for 60 min, at which point normal conditions were re-established for a further 15 min. Zero-calcium solutions were made up by excluding Ca^{2+} from the composition of aCSF and adding the calcium chelator EGTA at a concentration of 50 μM. IL-1β, TNF-α, IL-6, anti-TNF-α (used at 10 μg/ml), and IL-1 receptor antagonist (IL-1ra; used at 5 μg/ml) were purchased from R&D Systems. Catalase (250 U/ml) and 4-hydroxy-2,2,6,6-tetramethylpiperidinyloxy (TEMPO; 500 μM) were purchased

Department of Cell Physiology and Pharmacology, University of Leicester, Leicester, United Kingdom

Received for publication December 17, 2004. Accepted for publication April 20, 2005.

The costs of publication of this article were defrayed in part by the payment of page charges. This article must therefore be hereby marked *advertisement* in accordance with 18 U.S.C. Section 1734 solely to indicate this fact.

[1] This work was supported by National Institute of Neurological Disorders and Stroke Grant NS44875 (to R.F.).

[2] Address correspondence and reprint requests to Dr. Robert Fern, Department of Cell Physiology and Pharmacology, University of Leicester, P.O. Box 138, University Road, Leicester, U.K. LE1 9HN. E-mail address: RF34@le.ac.uk

[3] Abbreviations used in this paper: PVL, periventricular leukomalacia; aCSF, artificial cerebrospinal fluid; $[Ca^{2+}]_i$, intracellular Ca^{2+} concentration; RON, rat optic nerve; IL-1ra, IL-1 receptor antagonist; ROS, reactive organ species.

0022-1767/05/$02.00

from Calbiochem. Unless otherwise stated, all other chemicals were purchased from Sigma-Aldrich. Data are presented as the mean ± SEM, with statistical significance determined by ANOVA with the Tukey posttest (PRISM; GraphPad).

Intracellular Ca^{2+} concentration ($[Ca^{2+}]_i$) imaging

The low affinity, Ca^{2+}-sensitive dye Fura-FF was used for Ca^{2+} imaging to limit the extent of Ca^{2+}-buffering. 1 mM Fura-FF AM (Molecular Probes) stock solution was made in dry DMSO and 10% pluronic acid. RONs were incubated for 50 min at room temperature in aCSF containing 10 μM FURA-FF AM. RONs were maintained in hydrated 95% O_2/5% CO_2 atmosphere during the incubation period and were washed in aCSF before being mounted in the perfusion chamber. The ends of the optic nerves were fixed to a 22 × 40 mm glass coverslip with small amounts of cyanoacrylate glue, leaving the majority of the nerve completely free of glue (26). The coverslip was sealed onto a Plexiglas perfusion chamber (atmosphere chamber; Warner Instruments) with silicone grease. The aCSF was perfused through the chamber at a rate of 2–3 ml/min, with a fluid level of ~2 mm completely covering the RON. 95% O_2/5% CO_2 was blown over the aCSF at a rate of 0.3 L/min. The chamber was mounted on the stage of an Nikon Eclipse TE200 inverted epifluorescence microscope. Chamber temperature was maintained closely at 37°C with a flow-through feedback tubing heater (Warner Instruments) positioned immediately before the aCSF entered the chamber, and a feedback objective heater (Bioptechs) that warmed the objective to 37°C. This combination of heating systems regulated the temperature of the bath and cover slip to 37°C, as established periodically with a temperature probe.

Cells within the RON were illuminated at 340, 360, and 380 nm by Monochromator (Optoscan; Cairn Research), and images were collected at 520 nm using an appropriate filter set (Chroma Technology). Images were taken with a cooled CCD camera (CoolSNAP HQ; Roper Scientific) every 60 s. This low recording frequency limited any damaging effect of illumination on the cells and reduced dye bleaching over the long recording times that were used. Changes in 340:380 ratio were taken to indicate changes in $[Ca^{2+}]_i$ (27). The 360 intensity (isosbestic point) was monitored to assess the capacity of cells to retain dye. The sudden loss of 360 signal correlated with loss of cell membrane integrity and the release of dye into the extracellular space (see Ref. 26). Data were collected and stored with the image acquisition program Metafluor (Universal Imaging) running on Windows XP. Because of slow shifting of the preparation, cells were occasionally refocused during experiments. A small proportion of cells slowly drifted out of the focal plane and were discarded. Many of the experiments required long recording periods (190 min), which had a relatively low success rate due to dye fading and/or shifting of the preparation.

Dead cell counts

Ethidium bromide, a lipophobic nuclear dye that does not stain intact living cells, was used to stain nuclei of dead cells. RONs were dissected and placed in aCSF. The nerves were incubated for 180 min at 37°C in 1 ml of an experiment solution. RONs were maintained in hydrated 95% O_2/5% CO_2 atmosphere during the incubation period and were subsequently washed with fresh aCSF. RONs were then incubated for 10 min at room temperature with 0.5 nM ethidium bromide. RONs were then washed in aCSF and live-mounted on a Nikon LABOPHOT-2 epifluorescence microscope equipped with a 20× fluorescence objective and appropriate filter. Whole RON images (excluding the cut ends) were captured with a CCD camera, averaging 16 frames. Cell counting was performed blind using ImageJ (NIH). The mean number of dead cells found following exposure to any given condition was compared with the number seen in control RONs (180 min aCSF only), and are expressed as a percentage change relative to this level of control cell death.

LPS binding/immunohistochemistry

Whole P10 rat brains were dissected free, and RONs were dissected free and left on the optic chiasm, before fixation in 3% paraformaldehyde for 30 min at room temperature and mounting in Tissue Tec (Sakura). Sections (20 μm) were cut with a cryostat before mounting on slides. Fluorescently conjugated LPS, (LPS-Alexa Fluor 488, *E. coli*; Molecular Probes), was used to detect LPS binding (1 μg/ml in PBS). Sections were blocked for 60 min at room temperature with PBS containing 10% goat serum and 0.5% Triton X-100 before incubation in conjugated LPS for 120 min at room temperature. Sections were either simultaneously costained with monoclonal anti-glial fibrillary acidic protein (GFAP) conjugated to Cy3 (Sigma-Aldrich; 1:500 in PBS), or stained overnight at 5°C with isolectin IB4 conjugated to Alexa-Fluor 594 (Molecular Probes; 1:100 in PBS). Sections were washed briefly after incubation in LPS-conjugate before fixation with 4% formaldehyde for 30 min in PBS. Slices were then washed in PBS (2 × 15 min) and mounted on an Olympus IX70 inverted confocal microscope for image collection. Conjugated probes were used to eliminate cross-reactions and the specificity of LPS-conjugate binding was tested by displacement with unconjugated LPS (see *Results*). No bleed through of fluorescence was detected between channels.

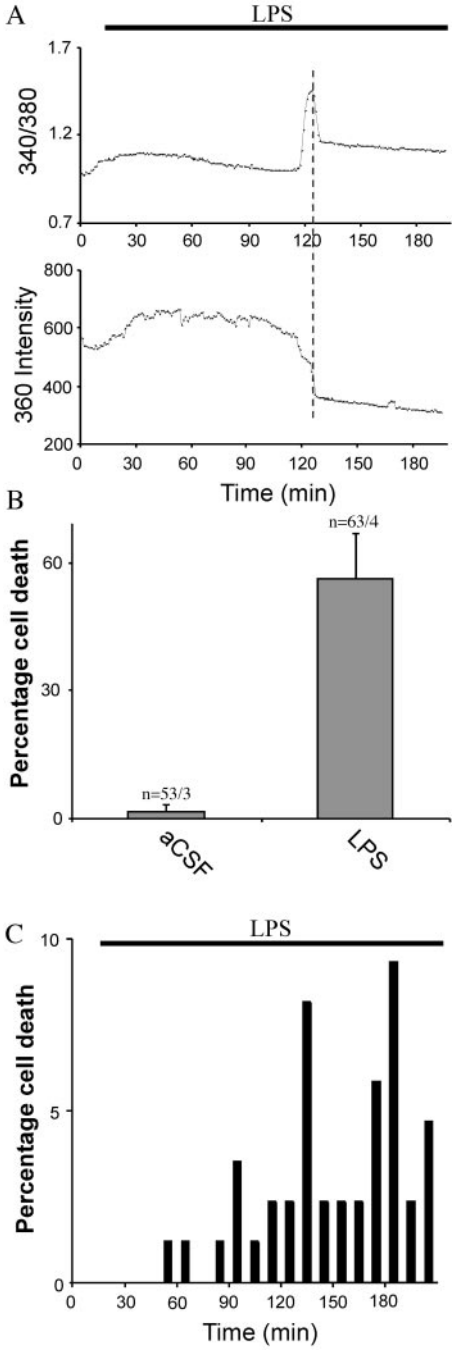

FIGURE 1. LPS induces $[Ca^{2+}]_i$ rises and subsequent cell death in neonatal white matter glia. *A*, Changes in the $[Ca^{2+}]_i$-dependent 340/380 ratio and $[Ca^{2+}]_i$-independent 360 intensity in a representative FURA-FF loaded glial cell within a RON perfused in aCSF + LPS (1 μg/ml) for 180 min. Following a period of control recording, exposure to LPS induced a delayed Ca^{2+} rise associated with cell death (dashed line). *B*, Degree of cell death during 180 min of control perfusion with aCSF and during 180 min of perfusion with LPS (n = cells/RONs). *C*, Time-course of cell death among the 64 cells that died following exposure to LPS, determined by loss of cytoplasmic FURA-FF and expressed as a percentage. Note the gradual increase in cell death with the period of LPS exposure, with death first becoming apparent after ~60–90 min.

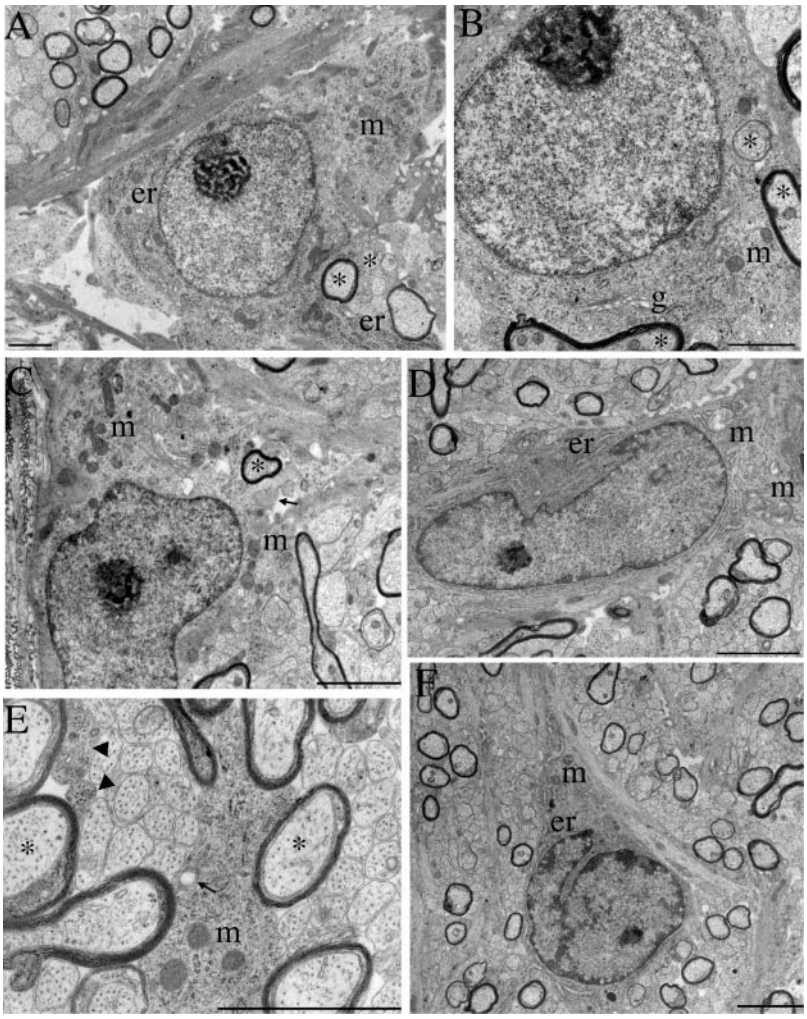

FIGURE 2. Ultrastructural changes evoked by LPS in the P10 RON. *A* and *B*, Control RON perfused with aCSF for 180 min postdissection. Typical immature oligodendrocytes are shown, characterized by the presence of myelinating and premyelinating axons embedded within the somata and processes ("*"), numerous mitochondria ("m"), a relatively narrow bore endoplasmic reticulum ("er"), and evenly dispersed chromatin within the nucleus that generally contained at least one prominent nucleolus (29). Golgi apparatus ("g") was often apparent. *C–F*, RON after 180 min LPS treatment. *C* and *D*, Typical LPS treated immature oligodendrocytes. The nuclear morphology is largely unaffected but mitochondria are either severely swollen or completely disrupted (*D*) and the cell membrane may be breached (note the free-floating distended mitochondria in *C*, arrow). Endoplasmic reticulum may also be distended, but gross cell swelling and wide-scale necrosis, such as that seen in postischemic neonatal RON glia (29), is not apparent. *E*, Mitochondrial damage is also evident in immature oligodendroglial processes (arrow). Note the healthy appearance of neighboring axons in *C–E*. *F*, Astrocyte in LPS treated RON. The endoplasmic reticulum is swollen but mitochondria are healthy and cell membrane is intact. Scale bar = 1 μm in all cases.

Electron microscopy

RONs were exposed to 1 μg/ml LPS in aCSF or control aCSF for 180 min before washing in Sorenson's buffer and postfixation in 3% glutaraldehyde/Sorenson's for 90 min at room temperature. The RONs were subsequently postfixed with 2% osmium tetroxide and dehydrated in ethanol and propylene oxide. The nerves were infiltrated in epoxy resin and the ends cut back before taking ultrathin sections. Sections were counterstained with uranyl acetate and lead citrate and examined with a JEOL 100CX electron microscope. To avoid bias in the data, electron micrographs were collected blind (by R. Fern) to the experimental procedure used to produce each sample.

Results

The 340/380 ($[Ca^{2+}]_i$-sensitive) ratio of FURA-FF loaded P10 RON glial cells was stable during control perfusion with aCSF for 190 min, with little cell death observed (1 of 53 cells, in 3 RONs). Following 10 min of control perfusion, glial cells in RONs exposed to LPS (1 μg/ml) generally had a stable $[Ca^{2+}]_i$ until a rapid rise preceded cell death in 59.4 $\pm$10.6% of cells (n = 63 cells, 4 RONs, $p < 0.001$: Fig. 1, *A* and *B*). The incidence of cell death tended to increase with the period of LPS exposure (Fig. 1*C*).

The P10 RON is at a similar developmental point to the human mid-term periventricular white matter that is subject to PVL (24, 25, 28). Ultrastructural examination of control RONs showed the typical components previously reported at this age: premyelinated axons and some early myelinated axons; astrocytes; and cells of the oligodendroglial lineage. Immature oligodendroglial cells could be

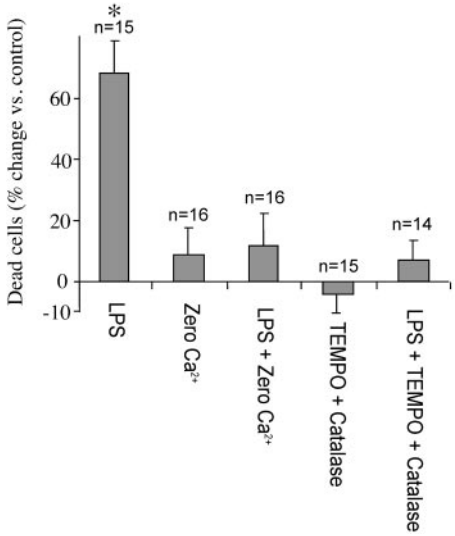

FIGURE 3. LPS-mediated acute cell death is Ca^{2+}- and ROS-dependent. Histogram showing the number of dead cells in RONs exposed to various experimental conditions, relative to control. LPS produced a significant increase in the number of dead cells in RONs, an effect that was blocked by removing extracellular Ca^{2+} or by the ROS scavengers TEMPO + catalase. RONs were incubated for 180 min in the various conditions, before ethidium bromide staining. Error bars = SEM, n = number of RONs; *, $p < 0.001$ vs control.

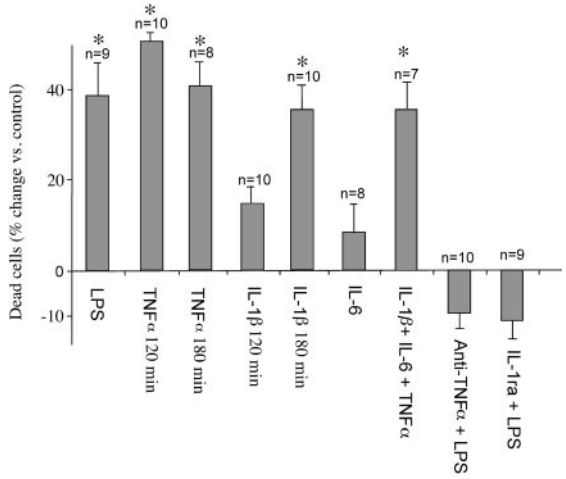

FIGURE 4. Cytokines mediate the cytotoxic effects of LPS. Histogram showing the number of dead cells in neonatal RON after 180 min of several experimental conditions, relative to control. A similar increase in the number of dead cells was apparent following 180 min exposure to LPS, TNF-α, IL-1β or TNF-α + IL-1β + IL-6. Although 120-min exposure to TNF-α was toxic, 120-min exposure IL-1β was not. IL-6 alone did not significantly increase the number of dead cells compared with control. Anti-TNF-α or IL-1ra blocked the cytotoxic effect of LPS. n = number of RONs, error bars = SEM; *, $p < 0.001$ vs control.

reliably identified by their characteristic nuclear morphology, narrow-bore endoplasmic reticulum and the presence of myelinated axons within the cell body or processes (29) (Fig. 1, *A* and *B*).

RONs subjected to 180 min of LPS treatment showed wide scale injury of immature oligodendrocytes (Fig. 2, *C* and *D*). Nuclear morphology appeared normal in these cells but mitochondria were swollen or ruptured and areas where the cell membrane had been lost could be identified in many cases. Similar changes were apparent in immature oligodendrocyte processes, although the degree of injury was less marked and cell membrane breakdown was not observed (Fig. 2*E*). No pathology was evident in axons, even those that were being ensheathed by immature oligodendrocytes that had died (Fig. 2*C*). Astrocytes were also largely unaffected in post-LPS treated RON (Fig. 2*F*).

The cytotoxic effect of LPS was confirmed by counting dead cells in P10 RONs following a standard 180 min exposure to 1 μg/ml LPS. RONs maintained in the presence of LPS had a 68.0 $\pm$ 10.2% increase in the number of dead cells compared with control ($p < 0.001$; Fig. 3). The cytotoxic effect of LPS was blocked by removing extracellular Ca^{2+} (+50 μM EGTA), or by addition of the reactive oxygen species (ROS) scavengers TEMPO + catalase (30) (Fig. 3). Neither zero Ca^{2+} nor ROS scavengers significantly affected the number of dead cells in the absence of LPS.

Cytokines are implicated as intermediaries in various bacterial infection models of white matter injury. Exposure for 180 min to the cytokines TNF-α (1,000 U/ml) or IL-1β (1,000 U/ml), but not IL-6 (1,000 U/ml), mimicked the cytotoxic effect of LPS (1 μg/ml) (Fig. 4). Exposure to all three cytokines (with IL-1β increased to 25,000 U/ml) had no additive cytotoxic effect (Fig. 4). Removing the biological activity of TNF-α by incubation in an inactivating Ab (10 μg/ml) abolished the cytotoxic action of LPS, as did incubation with an antagonist of IL-1, IL-1ra (5 μg/ml). Although

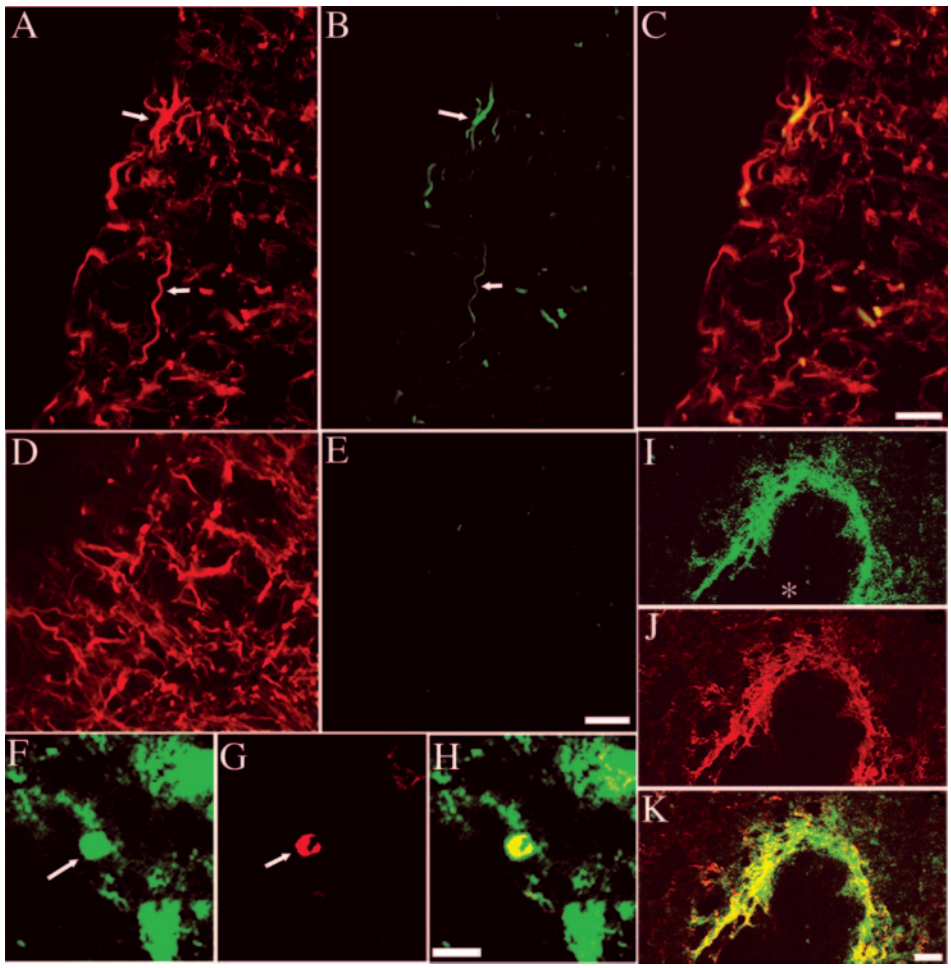

FIGURE 5. LPS-binding sites are present on both microglia and astrocytes in neonatal RON. *A*, GFAP staining of astrocytes in P10 RON. *B*, Conjugated LPS binding of the same section. *C*, Merge, showing LPS binding to astrocyte somata and processes (arrows). *D*, GFAP staining of astrocytes in P10 RON. *E*, Conjugated LPS binding of the same section, performed in the presence of a 10 times excess of unconjugated LPS. Note the absence of LPS binding. *F*, Conjugated LPS binding of P10 RON. *G*, Same section showing conjugated-isolectin B4 (IB4) binding on a microglial cell. *H*, Merge, showing coexpression of LPS and IB4 binding sites on the microglial cell (arrow). *I*, Conjugated LPS binding in a P10 brain slice, showing intense binding around a blood vessel (vessel lumen indicated by "*"). *J*, GFAP binding of the same section showing $GFAP^+$ astrocytes surrounding the blood vessel. *F*, Merge, showing intense LPS binding to the perivascular astrocytes. Bar = 10 μm in all cases.

120 min exposure to IL-1β was toxic, 120 min of IL-1β was not toxic.

To probe the site of action of LPS, conjugated LPS binding was examined in P10 RON and brain. LPS binding was widespread throughout P10 RON, colocalizing with GFAP$^+$ astrocyte somata and processes (Fig. 5, *A–C*). Conjugated LPS binding was displaced by coincubation with nonconjugated LPS (10 μg/ml) (Fig. 5, *D* and *E*), proving the selectivity of the binding. Microglial labeling with I-B4 revealed a sparse population of I-B4$^+$ cells that bound conjugated LPS (Fig. 5, *F–H*). These cells were rare, and the great majority of LPS binding cells were I-B4$^-$. Widespread binding of conjugated LPS was also found in P10 brain slices, again largely colocalized with GFAP$^+$ astrocytes. Binding in brain slices was particularly intense on astrocytes surrounding blood vessels (Fig. 5, *I–K*).

Several reports suggest that bacterial and ischemic injury may be additive in developing white matter (31). Consistent with our previous results, ischemic conditions evoked $[Ca^{2+}]_i$ rises associated with cell death in FURA-FF loaded P10 RON glia (Fig. 6, *A* and *B*), (29, 32). Qualitatively similar events were seen during ischemia in the presence of LPS (1 μg/ml) (Fig. 6, *C* and *D*), and the degree of cell death produced by ischemia was significantly higher in the presence of LPS (1 μg/ml) (Fig. 7).

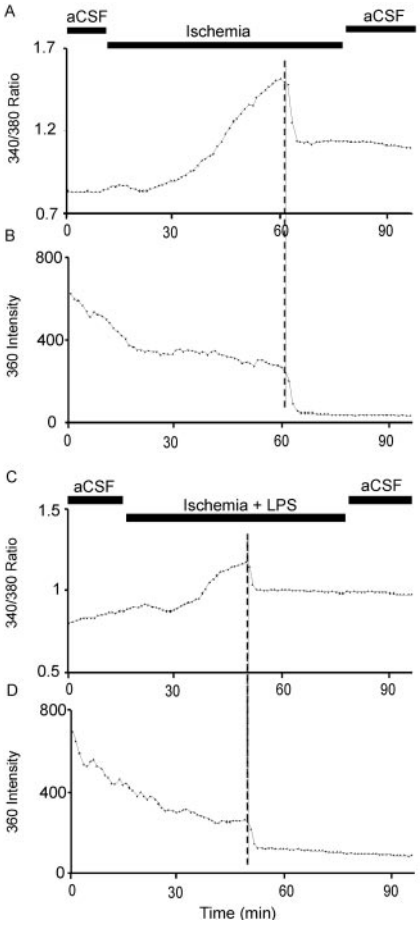

FIGURE 6. $[Ca^{2+}]_i$ changes and cell death in neonatal RON glial cells during ischemia: effect of LPS. *A*, $[Ca^{2+}]_i$-sensitive 340/380 ratio changes in a typical FURA-FF-loaded cell evoked by 60 min of ischemia (oxygen and glucose withdrawal). *B*, The accompanying 360 intensity changes, showing cell death (dashed line), which is associated with an elevation in $[Ca^{2+}]_i$. *C*, 340/380 ratio changes in a typical cell during 60 min of ischemia in the presence of LPS. *D*, Accompanying 360 intensity changes, showing cell death (dashed line).

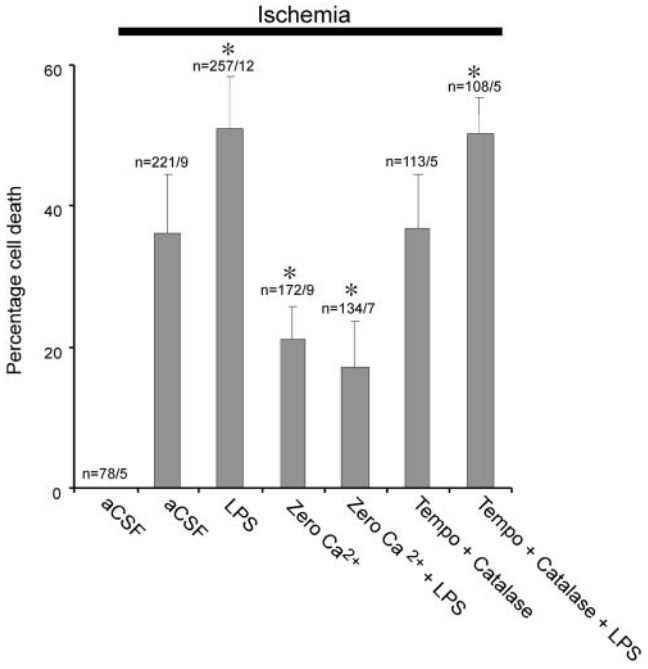

FIGURE 7. Histogram showing the incidence of cell death in ischemia experiments performed in various solutions, detected by loss of FURA-FF fluorescence. No cell death was found under control conditions (aCSF) over the 90 min period of the experiments. The degree of cell death found during ischemia was significantly higher when LPS (1 μg/ml) was included in the perfusing solution. Removing extracellular Ca^{2+} (+50 μM EGTA) significantly reduced the cell death evoked by ischemia and blocked the increase in ischemic cell death produced by LPS. The ROS scavengers TEMPO and catalase had no effect either upon the cell death produced by ischemia, or ischemia + LPS. Percentage cell death is calculated as the number of cells that died of the total number of cells for each experiment type. Error bars = SEM, n = total number of cells/number of RONs; *, $p < 0.01$ vs ischemia alone.

We have recently reported that removing extracellular Ca^{2+} is protective against oligodendroglial death, and increases astrocyte death during acute ischemia in the P10 RON (29, 32). The overall level of glial death during ischemia was significantly reduced by removing extracellular Ca^{2+} ($p < 0.01$), and the increase in cell death during ischemia produced by LPS was absent in zero-Ca^{2+} (Fig. 7). Unlike for the LPS-mediated cell death produced by 180 min of exposure to LPS, the additive effect of LPS upon ischemic cell death was not reduced by the ROS scavengers TEMPO + catalase (Fig. 7).

Discussion

Induction of maternal bacterial infection in rabbits can reproduce a focal and diffuse white matter injury in fetal brain that has some similarities to PVL (12, 13, 33). Intracerebral or ventricular injection of LPS in neonatal rat can also produce white matter damage (10, 11). The current study demonstrates LPS toxicity in immature white matter oligodendrocytes in a whole mount preparation. LPS is therefore directly and acutely toxic to developing white matter glia, irrespective of vascular factors that may come into play during infection (20). The rapid death of immature oligodendrocytes found in this preparation was not reported following exposure to LPS in cell culture (15, 16), suggesting that interactions between cell types in situ underlies the acute toxicity.

LPS binds to microglia and astrocytes in situ

TLR-4 (+CD14) is the only known binding site for LPS (34). Cell culture studies report that microglia express TLR-4, whereas oligodendrocyte precursors do not (17), and astrocytes either do not (17) or express very low levels unless pre-exposed to LPS (35). LPS binding has not previously been examined in situ. We report extensive LPS binding in neonatal RON and brain. LPS binding was particularly marked around blood vessels. Microglial cells were shown to bind LPS, but the majority of LPS-bindings cells were $GFAP^+$ astrocytes in both RON and brain. The acute cytotoxic effect of LPS upon immature oligodendrocytes is therefore mediated by other glial cell types, presumably mainly astrocytes.

LPS toxicity is delayed and is Ca^{2+} dependent

The acute cell death evoked by LPS reported in this study was preceded by a delayed sudden increase in $[Ca^{2+}]_i$ and was prevented by removing extracellular Ca^{2+}, demonstrating the Ca^{2+} dependence of the injury. The delayed nature of the $[Ca^{2+}]_i$ rise is consistent with LPS having initial effects on astrocytes and/or microglial cells, which then mediate a delayed and lethal rise in oligodendrocyte $[Ca^{2+}]_i$. If this is correct, the initial effects that precede the oligodendrocyte $[Ca^{2+}]_i$ rise take between 60 and 120 min and constitute the priming steps in an injury cascade.

The role of cytokines

The incidence of PVL in premature infants is correlated with elevated cytokine levels in umbilical cord blood, amniotic fluid and neonatal blood (33, 36, 37). We report that TNF-α and IL-1β directly evoke acute cell death in RON glia, with the degree of cell death not significantly different from that produced by LPS. Although implicated in the inflammatory response to LPS (38), IL-6 was not found to cause acute glial cell death. Combined IL-1β, IL-6, and TNF-α exposure did not increase the degree of cell death, and it appears that maximal injury was achieved at the cytokine concentrations used in this study.

LPS-mediated cell death was reduced to the level seen in control experiments by the addition of a neutralizing Ab for TNF-α, or of IL-1ra. Therefore, production of both cytokines is necessary for the acute cytotoxic effects of LPS. Maternal venous LPS injection elevates fetal brain TNF-α and IL-1β mRNA within 60 min (39). In cell culture, LPS can induce TNF-α release from microglia within 60–120 min and IL-1β within 120–180 min (the earliest time points measured) (40–43). Cultured astrocytes are also capable of cytokine release (44), with LPS-induced TNF-α release requiring the prior release of IL-1β (45–47). This is consistent with the current finding that 120 min of exposure to TNF-α was toxic but IL-1β required 180 min of exposure for toxicity to become apparent. If astrocytes are the major source of the cytokine release induced by LPS, as the LPS binding data would suggest, this would explain the protection provided by blocking either TNF-α or IL-1β.

LPS-stimulated production of glial TNF-α and IL-1β involves the activation of the transcription factor NF-κB, which is evident within 60 min of LPS exposure in cell culture (48). Cytokines and ROS are also strong activators of NF-κB in glia (48, 49), suggesting a feed-forward loop involving exposure to LPS, activation of NF-κB, cytokine and ROS generation and further activation of NF-κB (Fig. 8). This would be consistent with the protective effect of ROS scavengers seen in the results and with studies showing LPS evoked ROS generation in cultured microglia and astrocytes (48, 50–53).

The toxic effect of TNF-α upon oligodendroglia is well characterized (e.g., Refs. 18 and 54), and IL-1β toxicity of oligodendroglia has also been reported (55). It is unclear whether such toxicity is a direct pathway to the glial injury described in the current results, because TNF-α-mediated oligodendroglial cell death is thought to be slow. However, significant death of cultured rat oligodendroglia has been reported within 120 min of exposure to TNF-α (18), and the generally slower oligodendrocyte death seen in other studies may be due to the low sensitivity to TNF-α-mediated injury in the mature cells used (54). However, a direct contribution of ROS to the oligodendroglial injury cannot be ruled out.

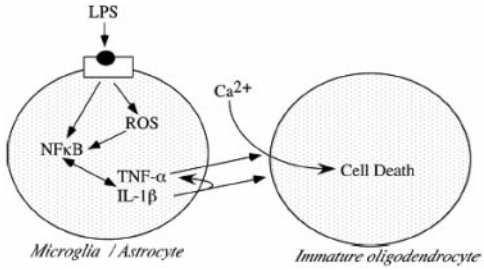

FIGURE 8. Summary, showing the current results and some known interactions between LPS, NFκB, ROS, and cytokine production in glia. LPS, (presumably acting at TLR-4), activates a cascade involving ROS generation, NF-κB and cytokine production in astrocytes and/or microglia. IL-1β required for subsequent TNF-α release from astrocytes. Cytokines are released into the extracellular space where they mediate the rapid rise influx of Ca^{2+} into immature oligodendrocytes and acute cell death.

LPS and ischemia

Prior reports suggest that bacterial endotoxin- and ischemia-mediated immature white matter injury is additive (31). Bacterial endotoxins such as LPS evoke hypotension and can be predicted to induce ischemia in fetal white matter in vivo (19, 20). The current study shows additive injury by LPS and ischemia in isolated immature white matter, independent of any hemodynamic factors that may come into play in vivo. This additive effect was Ca^{2+} dependent; whereas both LPS- and ischemia-induced injury of RON oligodendrocytes is mediated by Ca^{2+} influx (29). However, the potentiation of ischemic injury by LPS occurred over a shorter time course (60 min) than was required for direct LPS toxicity, and was not affected by ROS scavengers that blocked direct toxicity. Therefore, it may be that interactions between LPS and ischemia involve different pathways than those operating during direct LPS toxicity.

Disclosures

The authors have no financial conflict of interest.

References

1. Volpe, J. J. 1995. *Neurology of the newborn.* W. B. Saunders, Philadelphia.
2. Volpe, J. J. 2001. Neurobiology of periventricular leukomalacia in the premature infant. *Pediatr. Res.* 50: 553–562.
3. Kinney, H. C., and S. A. Back. 1998. Human oligodendroglial development: relationship to periventricular leukomalacia. *Semin. Pediatr. Neurol.* 5: 180–189.
4. Back, S. A., N. L. Luo, N. S. Borenstein, J. M. Levine, J. J. Volpe, and H. C. Kinney. 2001. Late oligodendrocyte progenitors coincide with the developmental window of vulnerability for human perinatal white matter injury. *J. Neurosci.* 21: 1302–1312.
5. Flodmark, O., B. Lupton, D. Li, G. K. Stimac, E. H. Roland, A. Hill, M. F. Whitfield, and M. G. Norman. 1989. MR imaging of periventricular leukomalacia in childhood. *AJR Am. J. Roentgenol.* 152: 583–590.
6. van de Bor, M., G. L. Guit, A. M. Schreuder, J. Wondergem, and G. J. Vielvoye. 1989. Early detection of delayed myelination in preterm infants. *Pediatrics* 84: 407–411.
7. Back, S. A., B. H. Han, N. L. Luo, C. A. Chricton, S. Xanthoudakis, J. Tam, K. L. Arvin, and D. M. Holtzman. 2002. Selective vulnerability of late oligodendrocyte progenitors to hypoxia-ischemia. *J. Neurosci.* 22: 455–463.
8. Gilles, F. H., A. Leviton, and C. S. Kerr. 1976. Endotoxin leucoencephalopathy in the telencephalon of the newborn kitten. *J. Neurol. Sci.* 27: 183–191.
9. Gilles, F. H., D. R. Averill, Jr., and C. S. Kerr. 1977. Neonatal endotoxin encephalopathy. *Ann. Neurol.* 2: 49–56.

10. Kong, G. Y., K. Kristensson, and M. Bentivoglio. 2002. Reaction of mouse brain oligodendrocytes and their precursors, astrocytes and microglia, to proinflammatory mediators circulating in the cerebrospinal fluid. *Glia* 37: 191–205.
11. Cai, Z., Y. Pang, S. Lin, and P. G. Rhodes. 2003. Differential roles of tumor necrosis factor-α and interleukin-1β in lipopolysaccharide-induced brain injury in the neonatal rat. *Brain Res.* 975: 37–47.
12. Debillon, T., C. Gras-Leguen, V. Verielle, N. Winer, J. Caillon, J. C. Roze, and P. Gressens. 2000. Intrauterine infection induces programmed cell death in rabbit periventricular white matter. *Pediatr. Res.* 47: 736–742.
13. Yoon, B. H., C. J. Kim, R. Romero, J. K. Jun, K. H. Park, S. T. Choi, and J. G. Chi. 1997. Experimentally induced intrauterine infection causes fetal brain white matter lesions in rabbits. *Am. J. Obstet. Gynecol.* 177: 797–802.
14. Merrill, J. E., L. J. Ignarro, M. P. Sherman, J. Melinek, and T. E. Lane. 1993. Microglial cell cytotoxicity of oligodendrocytes is mediated through nitric oxide. *J. Immunol.* 151: 2132–2141.
15. Pang, Y., Z. Cai, and P. G. Rhodes. 2000. Effects of lipopolysaccharide on oligodendrocyte progenitor cells are mediated by astrocytes and microglia. *J. Neurosci. Res.* 62: 510–520.
16. Molina-Holgado, E., J. M. Vela, A. Arevalo-Martin, and C. Guaza. 2001. LPS/IFN-γ cytotoxicity in oligodendroglial cells: role of nitric oxide and protection by the anti-inflammatory cytokine IL-10. *Eur. J. Neurosci.* 13: 493–502.
17. Lehnardt, S., C. Lachance, S. Patrizi, S. Lefebvre, P. L. Follett, F. E. Jensen, P. A. Rosenberg, J. J. Volpe, and T. Vartanian. 2002. The Toll-like receptor TLR4 is necessary for lipopolysaccharide-induced oligodendrocyte injury in the CNS. *J. Neurosci.* 22: 2478–2486.
18. Robbins, D. S., Y. Shirazi, B. E. Drysdale, A. Lieberman, H. S. Shin, and M. L. Shin. 1987. Production of cytotoxic factor for oligodendrocytes by stimulated astrocytes. *J. Immunol.* 139: 2593–2597.
19. Young, R. S., M. J. Hernandez, and S. K. Yagel. 1982. Selective reduction of blood flow to white matter during hypotension in newborn dogs: a possible mechanism of periventricular leukomalacia. *Ann. Neurol.* 12: 445–448.
20. Yanowitz, T. D., J. A. Jordan, C. H. Gilmour, R. Towbin, A. Bowen, J. M. Roberts, and B. S. Brozanski. 2002. Hemodynamic disturbances in premature infants born after chorioamnionitis: association with cord blood cytokine concentrations. *Pediatr. Res.* 51: 310–316.
21. Follett, P. L., P. A. Rosenberg, J. J. Volpe, and F. E. Jensen. 2000. NBQX attenuates excitotoxic injury in developing white matter. *J. Neurosci.* 20: 9235–9241.
22. Fern, R., and T. Moller. 2000. Rapid ischemic cell death in immature oligodendrocytes: a fatal glutamate release feedback loop. *J. Neurosci.* 20: 34–42.
23. Foster, R. E., B. W. Connors, and S. G. Waxman. 1982. Rat optic nerve: electrophysiological, pharmacological and anatomical studies during development. *Brain Res.* 255: 371–386.
24. Vaughn, J. E. 1969. An electron microscopic analysis of gliogenesis in rat optic nerves. *Z Zellforsch Mikrosk Anat.* 94: 293–324.
25. Craig, A., N. Ling Luo, D. J. Beardsley, N. Wingate-Pearse, D. W. Walker, A. R. Hohimer, and S. A. Back. 2003. Quantitative analysis of perinatal rodent oligodendrocyte lineage progression and its correlation with human. *Exp. Neurol.* 181: 231–240.
26. Fern, R. 1998. Intracellular calcium and cell death during ischemia in neonatal rat white matter astrocytes in situ. *J. Neurosci.* 18: 7232–7243.
27. Grynkiewicz, G., M. Poenie, and R. Y. Tsien. 1985. A new generation of Ca^{2+} indicators with greatly improved fluorescence properties. *J. Biol. Chem.* 260: 3440–3450.
28. Skoff, R. P., D. L. Price, and A. Stocks. 1976. Electron microscopic autoradiographic studies of gliogenesis in rat optic nerve. II. Time of origin. *J. Comp. Neurol.* 169: 313–334.
29. Wilke S, Salter M, Thomas R, Allcock N, and Fern R. Mechanism of acute ischemic injury of oligodendroglia in early myelinating white matter: the importance of astrocyte injury and glutamate release. *J. Neurol. Exp. Neuropath.* 63: 872–881.
30. Vergun, O., A. I. Sobolevsky, M. V. Yelshansky, J. Keelan, B. I. Khodorov, and M. R. Duchen. 2001. Exploration of the role of reactive oxygen species in glutamate neurotoxicity in rat hippocampal neurones in culture. *J. Physiol.* 531: 147–163.
31. Hagberg, H., D. Peebles, and C. Mallard. 2002. Models of white matter injury: comparison of infectious, hypoxic-ischemic, and excitotoxic insults. *Ment. Retard. Dev. Disabil. Res. Rev.* 8: 30–38.
32. Thomas, R., Wilke S, Husen A, Allcock N, Nivison M, Nnoli A N, and R. Fern. Acute ischemic injury of astrocytes is mediated by Na-K-Cl cotransport and not Ca^{2+} influx at a key point in white matter development. *J. Neuropathol. Exp. Neurol. In press*.
33. Yoon, B. H., C. W. Park, and T. Chaiworapongsa. 2003. Intrauterine infection and the development of cerebral palsy. *BJOG* 110(Suppl. 20): 124–127.
34. Raetz, C. R., and C. Whitfield. 2002. Lipopolysaccharide endotoxins. *Annu. Rev. Biochem.* 71: 635–700.
35. Bowman, C. C., A. Rasley, S. L. Tranguch, and I. Marriott. 2003. Cultured astrocytes express toll-like receptors for bacterial products. *Glia* 43: 281–291.
36. Grether, J. K., K. B. Nelson, E. S. Emery III, and S. K. Cummins. 1996. Prenatal and perinatal factors and cerebral palsy in very low birth weight infants. *J. Pediatr.* 128: 407–414.
37. Nelson, K. B., J. M. Dambrosia, J. K. Grether, and T. M. Phillips. 1998. Neonatal cytokines and coagulation factors in children with cerebral palsy. *Ann. Neurol.* 44: 665–675.
38. Yoon, B. H., R. Romero, J. K. Jun, K. H. Park, J. D. Park, F. Ghezzi, and B. I. Kim. 1997. Amniotic fluid cytokines (interleukin-6, tumor necrosis factor-α, interleukin-1β, and interleukin-8) and the risk for the development of bronchopulmonary dysplasia. *Am. J. Obstet. Gynecol.* 177: 825–830.
39. Cai, Z., Z. L. Pan, Y. Pang, O. B. Evans, and P. G. Rhodes. 2000. Cytokine induction in fetal rat brains and brain injury in neonatal rats after maternal lipopolysaccharide administration. *Pediatr. Res.* 47: 64–72.
40. Ogata, T., M. Chuai, T. Morino, H. Yamamoto, Y. Nakamura, and P. Schubert. 2003. Adenosine triphosphate inhibits cytokine release from lipopolysaccharide-activated microglia via P2y receptors. *Brain Res.* 981: 174–183.
41. Liu, B., K. Wang, H. M. Gao, B. Mandavilli, J. Y. Wang, and J. S. Hong. 2001. Molecular consequences of activated microglia in the brain: overactivation induces apoptosis. *J. Neurochem.* 77: 182–189.
42. Sanz, J. M., and F. Di Virgilio. 2000. Kinetics and mechanism of ATP-dependent IL-1β release from microglial cells. *J. Immunol.* 164: 4893.
43. Chauvet, N., K. Palin, D. Verrier, S. Poole, R. Dantzer, and J. Lestage. 2001. Rat microglial cells secrete predominantly the precursor of interleukin-1β in response to lipopolysaccharide. *Eur. J. Neurosci.* 14: 609–617.
44. Dong, Y., and E. N. Benveniste. 2001. Immune function of astrocytes. *Glia* 36: 180–190.
45. Lee, S. C., W. Liu, D. W. Dickson, C. F. Brosnan, and J. W. Berman. 1993. Cytokine production by human fetal microglia and astrocytes: differential induction by lipopolysaccharide and IL-1β. *J. Immunol.* 150: 2659–2667.
46. Lee, S. C., D. W. Dickson, W. Liu, and C. F. Brosnan. 1993. Induction of nitric oxide synthase activity in human astrocytes by interleukin-1β and interferon-γ. *J. Neuroimmunol.* 46: 19–24.
47. Park, J., D. Kwon, C. Choi, J. W. Oh, and E. N. Benveniste. 2003. Chloroquine induces activation of nuclear factor-κB and subsequent expression of pro-inflammatory cytokines by human astroglial cells. *J. Neurochem.* 84: 1266.
48. Possel, H., H. Noack, J. Putzke, G. Wolf, and H. Sies. 2000. Selective upregulation of inducible nitric oxide synthase (iNOS) by lipopolysaccharide (LPS) and cytokines in microglia: in vitro and in vivo studies. *Glia* 32: 51–59.
49. Akama, K. T., and L. J. Van Eldik. 2000. β-Amyloid stimulation of inducible nitric-oxide synthase in astrocytes is interleukin-1β- and tumor necrosis factor-α (TNFα)-dependent, and involves a TNFα receptor-associated factor- and NFκB-inducing kinase-dependent signaling mechanism. *J. Biol. Chem.* 275: 7918–7924.
50. Wang, T., L. Qin, B. Liu, Y. Liu, B. Wilson, T. E. Eling, R. Langenbach, S. Taniura, and J. S. Hong. 2004. Role of reactive oxygen species in LPS-induced production of prostaglandin E_2 in microglia. *J. Neurochem.* 88: 939–947.
51. Faggioni, R., S. Gatti, M. T. Demitri, R. Delgado, B. Echtenacher, P. Gnocchi, H. Heremans, and P. Ghezzi. 1994. Role of xanthine oxidase and reactive oxygen intermediates in LPS- and TNF-induced pulmonary edema. *J. Lab. Clin. Med.* 123: 394–399.
52. Nakamura, Y., Q. S. Si, and K. Kataoka. 1999. Lipopolysaccharide-induced microglial activation in culture: temporal profiles of morphological change and release of cytokines and nitric oxide. *Neurosci. Res.* 35: 95–100.
53. Calabrese, V., A. Copani, D. Testa, A. Ravagna, F. Spadaro, E. Tendi, V. G. Nicoletti, and A. M. Giuffrida Stella. 2000. Nitric oxide synthase induction in astroglial cell cultures: effect on heat shock protein 70 synthesis and oxidant/antioxidant balance. *J. Neurosci. Res.* 60: 613–622.
54. Scurlock, B., and G. Dawson. 1999. Differential responses of oligodendrocytes to tumor necrosis factor and other pro-apoptotic agents: role of ceramide in apoptosis. *J. Neurosci. Res.* 55: 514–522.
55. Takahashi, J. L., F. Giuliani, C. Power, Y. Imai, and V. W. Yong. 2003. Interleukin-1β promotes oligodendrocyte death through glutamate excitotoxicity. *Ann. Neurol.* 53: 588–595.